

Performance Evaluation of Time Hopping UWB Transmission Using S-Rake Receiver

SAID GHENDIR ⁽¹⁾⁽²⁾, SALIM SBAA ⁽¹⁾, RIADH AJGOU ⁽¹⁾, ALI CHEMSA ⁽¹⁾, and A. TALEB-AHMED ⁽³⁾

⁽¹⁾ LI3CUB Laboratory, Electric Engineering Department
University of Biskra
B.P 145 R.P, 07000 Biskra
ALGERIA

⁽²⁾ Department of Sciences and Technology
El-Oued University
PO Box 789 39000 El-Oued
ALGERIA

⁽³⁾ LAMIH Laboratory
Valenciennes University
UVHC - Mont Houy - 59313 Valenciennes Cedex 9
FRANCE

said-ghendir@univ-eloued.dz, s.sbaa@univ-biskra.dz, riadh-ajgou@univ-eloued.dz,
chemsadoct@yahoo.fr, abdelmalik.talebahmed@univ-valenciennes.fr

Abstract: - In this paper, we address a performance evaluation of Time Hopping Ultra-Wideband (TH-UWB) transmission with proposed procedures, based on Pulse Position Modulation (PPM) and considering IEEE 802.15.3a Channel Models (CM1, CM2, CM3, CM4). Moreover, a Selective Rake (S-Rake) receiver is designed to counter the effects of multipath fading occurring in UWB channel Models. The TH-UWB signal detection through the S-Rake receiver requires a channel estimation which is done here using Maximum-Likelihood (ML) approach, and via two methods, Data Added (DA) and Non-Data Added (NDA). Important comparisons based on simulation results of UWB channel models, estimation methods, and multiuser access detection have been done. Finally, the MSE of the estimated channel parameters and the BER versus SNR are both assessed and discussed.

Key-Words: - Channel Estimation, DA, ML, NDA, PPM, S-Rake, TH-UWB.

1 Introduction

Ultra-WideBand transmission is an emerging technique for very high speed wireless communications. The UWB signals operate at an extremely wide range of frequencies from 3.1 GHz up to 10.6 GHz and allow high rate data transmission, which is expected to reach above 2 Gbits/s with low power consumption [1]. In the future, the UWB technology that consumes low electricity is applied to many portable devices [2]. Besides, it is based on transmitting pulses with a very short period that imposes in frequency domain an Ultra-Wideband [3].

Elsewhere, the IEEE 802.15.3a task group has set out four channel models (CM1, CM2, CM3, CM4) to define the UWB physical layer with specified characteristics [4]. Moreover, the rake receiver works well in a multipath environment, but

it requires knowledge of the multipath gains and the multipath delays, which are obtained using channel estimators. Thus, estimation becomes an important issue. The Rake receiver is known as a technique that can effectively combine paths with different delays and obtain the path diversity gain [5]. A way to utilize the appropriate multipath components in UWB environment is to use the Selective-Rake receiver, which combines the strongest signal components that have propagated through the channel by different paths. This can be characterized as a type of time diversity. The combination of different signal components will increase the SNR, which will improve the transmission performances.

In [6], a robust receiver design incorporating a channel estimation scheme is introduced, where a combined adaptive Rake and equalizer structure are used to reduce intense multi-path. Maximum-

likelihood channel estimation approach is developed in [7] under the presence of multiple-access interference (MAI) which is thought of as a white Gaussian process. In [8], a simple "sliding window" and "successive cancellation" algorithms are considered as a practical channel estimation scheme in a single-user, where a comparison between direct-sequence and time-hopping has been made. A more realistic UWB channel model proposed by IEEE 802.15.3a group has been adopted in [9]. In [10], channel estimation and signal detection for UWB communications have been investigated with Minimum Mean Square Estimation (MMSE) rake receiver at 7.5 GHz frequency.

The purpose of this paper is to propose some procedures in order to increase the performances of TH-UWB transmission. In addition, we aim to compare important parameters in terms of channel models and estimation methods, while avoiding complicated approaches, mainly in the case of multiuser and high bit rate. Our proposed procedures is to apply the ML approach as in [7], but with channel models adopted by IEEE 802.15.3a group. Moreover, in order to make the signal processing system as simple as possible, we will use a simple impulse shape, which is "monocycle" the first derivative of a Gaussian impulse. Moreover, we will exploit the S-Rake receiver type, and only the multipath components that are within 10 dB of the peak amplitude will be taken into consideration during the detection.

This paper is organized as follows. Section 2 gives an introduction to the TH-UWB signal format and S-Rake receiver. In section 3, IEEE 802.15.3a standard is presented to describe the UWB channel models. Furthermore, UWB channel estimation from the received waveform is provided by applying the ML approach, and under two methods, DA and NDA. Section 4 provides simulation results to show performances of TH-UWB transmission under our assumptions.

2 TH-UWB Signal Format and S-Rake Receiver

A typical TH-UWB transmitted signal with pulse position modulation (PPM) for the n^{th} user is given by

$$s_n(t) = \sum_k b(t - kN_f T_f - \delta a_k) \quad (1)$$

Where, one bit is

$$b(t) = \sum_{j=0}^{N_f-1} w(t - jT_f - c_j T_c) \quad (2)$$

In the last equation $w(t)$ is the pulse shape that nominally begins at time zero on the transmitter clock; and T_f is the frame time, i.e., N_f is a number of frames in one bit. The sequence $\{c_j\}$ is the user's time-hopping code and its elements are integers taking values in the range $0 < c_j < N_c - 1$; where, N_c is a number of chips in one frame; the parameter T_c is the duration of the chip.

From equation (1), a_k represents the data bits that has a duration T_b and is modeled as binary (0 or 1), independent and identically distributed (i.i.d.) random variables. Correspondingly, δ is a modulation factor for PPM modulation and the parameter T_w is the monocycle duration. Intuitively, increasing the duty cycle reduces the MAI (Multiple Access Interference) and improves the system performance [11].

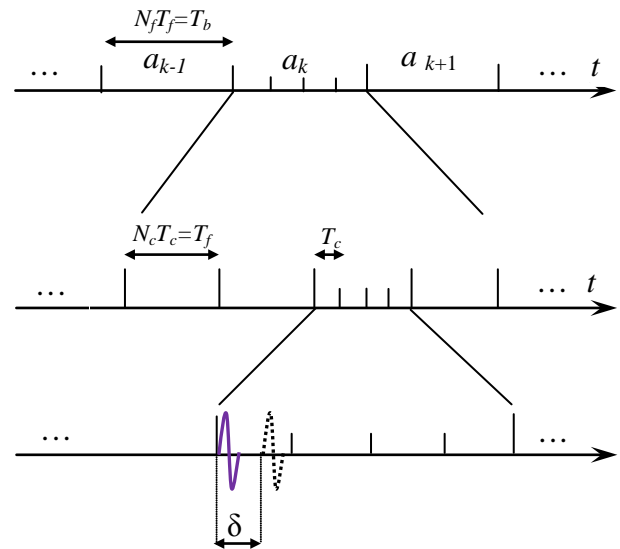


Fig.1 Structure of TH-UWB signal for PPM modulation

We have chosen the monocycle shape designed by the following relation:

$$w(t) = \left(\frac{t - T_w/2}{T_w} \right) \exp \left[- \left(\frac{t - T_w/2}{T_w} \right)^2 \right] \quad (3)$$

The output signal of the receiver antenna given by

$$r(t) = \sum_{l=0}^{L_c} \alpha_l s(t - \tau_l) + v(t) + u(t) \quad (4)$$

Where, $r(t)$ is the desired user's signal, α_l and τ_l are the attenuation, and the delay affecting its replica traveling through the l^{th} path, $v(t)$ is thermal noise and $u(t)$ represents the MAI caused by the other users. Assuming that The MAI is thought of as a white Gaussian process [10] and as such, it can be lumped into the thermal noise in (4), consequently we can write:

$$r(t) = \sum_{l=0}^{L_c} \alpha_l s(t - \tau_l) + n(t) \quad (5)$$

Where, $n(t) = v(t) + u(t)$ is still a Gaussian and white process. In order to exploit the multipath diversity existing in the received signal, the S-Rake receiver with L_c fingers is used. Where, in our case the paths that are within 10 dB of the peak amplitude will be captured by fingers.

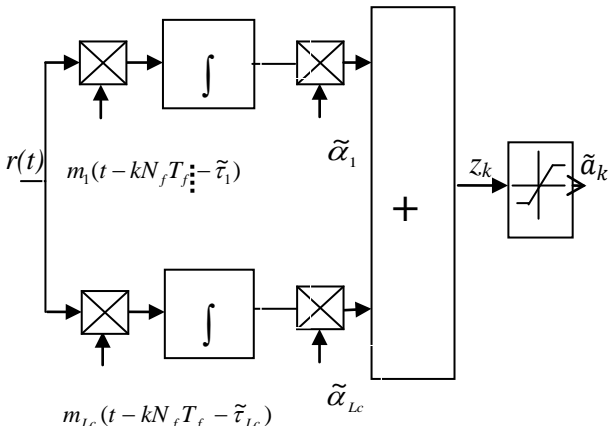


Fig.2 Block diagram of S-Rake receiver

The decision statistic is the maximal-ratio combination of the outputs of the correlators [13]:

$$z_k = \sum_{l=1}^{L_c} \alpha_l \int_{kN_f T_f}^{(k+1)N_f T_f} r(t) m(t - kN_f T_f - \tau_l) dt \quad (6)$$

Where, the template signal $m(t) = b(t) - b(t - \delta)$ depends not only on the user's time hopping code, but also on $w(t)$. In practice, the parameters α_l and τ_l are not known a priori and must be estimated.

3 IEEE 802.15.3a Channel Models

The IEEE UWB channel model is based on the Saleh-Valenzuela model where multipath components arrive in clusters [14], as the channel measurements showed multipath arriving in clusters. This is partly a result of the very fine resolution that ultra-wideband waveforms provide.

The IEEE 802.15.3a measurements, taken in the UWB band, observe a lognormal distribution for multipath fading; this distribution fits the measurements better than both the Rayleigh. The model also statistically characterizes the multipath arrival times, thus providing a double exponential decay.

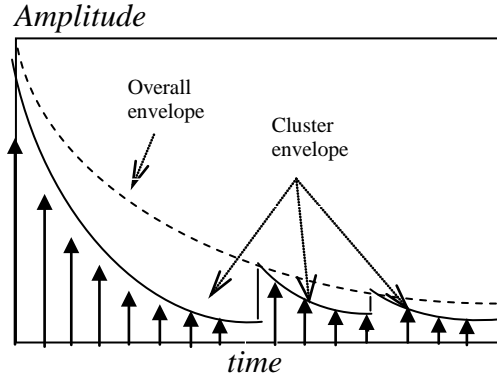


Fig.3 An illustration of double exponential decay

The multipath channel can be expressed as

$$h(t) = X \sum_{l=0}^L \sum_{q=0}^q \alpha_{q,l} \delta(t - T_l - \tau_{q,l}) \quad (7)$$

- X : represents the log-normal shadowing
- $\alpha_{q,l}$: are the multipath gain coefficients
- T_l : is the delay of the l^{th} cluster
- $\tau_{q,l}$: is the delay of the q^{th} multipath component relative to the l^{th} cluster

The distribution of cluster arrival time and the ray arrival time are given by

$$p(T_l | T_{l-1}) = \Lambda \exp[-\Lambda(T_l - T_{l-1})], \quad l > 0 \quad (8)$$

$$p(\tau_{q,l} | \tau_{(q-1),l}) = \lambda \exp[-\lambda(\tau_{q,l} - \tau_{(q-1),l})], \quad k \quad (9)$$

Where

- Λ : cluster arrival rate
- λ : ray arrival rate, i.e. the arrival rate of path within each cluster

The channel coefficients are log-normally distributed defined as follows

$$\alpha_{q,l} = p_{q,l} \xi_l \beta_{q,l} \quad (10)$$

The amplitude statistics of the measurements were found to best fit the log-normal distribution. In addition, the large-scale fading is also log-normally distributed.

$$20\log_{10}(\xi_l \beta_{q,l}) \propto \text{Normal}(\mu_{q,l}, \sigma_1^2 + \sigma_2^2) \quad (11)$$

$$\Rightarrow |\xi_l \beta_{q,l}| = 10^{(\mu_{q,l} + n_1 + n_2)/20} \quad (12)$$

Where

$$n_1 \propto \text{Normal}(0, \sigma_1^2) \quad (13)$$

And

$$n_2 \propto \text{Normal}(0, \sigma_2^2) \quad (14)$$

n_1, n_2 are independent and correspond to the fading on each cluster and ray, respectively. The averaged power delay profile is given by:

$$E\left[|\xi_l \beta_{q,l}|^2\right] = \Omega_0 e^{-T_l/\Gamma} e^{-\tau_{q,l}/\gamma} \quad (15)$$

This reflects the exponential decay of each cluster, as well as the decay of the total cluster power with delay.

$B_{q,l}$ in (10) is equiprobable +/-1 to account for signal inversion due to reflections. The $\mu_{q,l}$ is given by:

$$\mu_{q,l} = \frac{10\ln(\Omega_0) - 10T_l/\Gamma - 10\tau_{q,l}/\gamma - (\sigma_1^2 + \sigma_2^2)\ln(10)}{\ln(10)} \quad (16)$$

In the above equations, ξ_l reflects the fading associated with the l^{th} cluster, and $\beta_{q,l}$ corresponds to the fading associated with the q^{th} ray of the l^{th} cluster.

Finally, since the log-normal shadowing of the total multipath energy is captured by the term X , the total energy contained in the terms $\alpha_{q,l}$ is normalized to unity for each realization. This shadowing term is characterized by the following:

$$20\log_{10}(X) \propto \text{Normal}(0, \sigma_x^2) \quad (17)$$

The model parameters were designed to fit measurement results. Four different measurement environments were defined, namely CM1, CM2, CM3, and CM4. CM1 describes a LOS (line-of-sight) scenario with a separation between transmitter and receiver of less than 4m. CM2 describes the same range, but for a Non-LOS situation. CM3 describes a Non-LOS scenario for distances between

transmitter and receiver 4-10m. Scenario 4 finally describes an environment with strong delay dispersion, resulting in a delay spread of 25ns.

3.1 Data-Aided Estimation

This estimation is based on using a_k known pilot bits in each packet to estimate the channel impulse response, and the received waveform is observed over an interval $0 < t < T_0$, with $T_0 = MT_b$.

The equation (5) ignores the structure of the MAI [15]. The parameters to be estimated are $\alpha = (\alpha_1, \alpha_2 \dots \alpha_{Lc})$ and $\tau = (\tau_1, \tau_2 \dots \tau_{Lc})$, where, the number of paths Lc is taken as a known quantity.

$$\tilde{s}(t) = \sum_{l=1}^{Lc} \tilde{\alpha}_l s(t - \tilde{\tau}_l) \quad (18)$$

The log-likelihood function of the pair (α, τ) takes the form [16]:

$$\log[\Lambda(\tilde{\alpha}, \tilde{\tau})] = 2 \int_0^{T_0} r(t) \tilde{s}(t) dt - \int_0^{T_0} \tilde{s}^2(t) dt \quad (19)$$

A more convenient expression is obtained substituting (18) into (19) and neglecting the correlation between signal echoes, i.e., assuming:

$$\frac{\int_0^{T_0} s(t - \tilde{\tau}_{l_1}) s(t - \tilde{\tau}_{l_2}) dt}{\int_0^{T_0} s(t) dt} \approx 0 \quad l_1 \neq l_2 \quad (20)$$

By performing some ordinary manipulations, we get:

$$\log[\Lambda(\tilde{\alpha}, \tilde{\tau})] = 2 \sum_{l=1}^{Lc} \tilde{\alpha}_l \sum_{k=0}^{M-1} z_k(\tilde{\tau}_l, a_k) - ME_b \sum_{l=1}^{Lc} \tilde{\alpha}_l^2 \quad (21)$$

Where, E_b is the energy of $b(t)$

It is clear that $z_k(\tilde{\tau}_l, a_k)$ are sufficient statistics to calculate the estimated parameters, and it is the response of the correlation between the received signal and the matched filter $b(-t)$ at $t = kNT_f + \delta a_k + \tilde{\tau}_l$.

The DA estimation is based on searching the peaks in the output of $z_k(\tilde{\tau}_l, a_k)$. Subsequently, by doing some manipulations, the multipath gain coefficients are given by:

$$\tilde{\alpha}_l = \arg \max \frac{1}{ME_b} J(\tilde{\tau}_l) \quad , \quad 1 \leq l \leq Lc \quad (22)$$

With

$$J(\tilde{\tau}) = \sum_{k=0}^{M-1} z_k(\tilde{\tau}, a_k) \quad (23)$$

In order to reach the delays τ_l it is sufficient to maximize the following formula to look the locations of the maximal values of $J(\tilde{\tau})$.

$$\sum_{l=1}^{Lc} J^2(\tilde{\tau}_l) \quad (24)$$

3.2 NON Data-Aided Estimation

In this case, the transmitted data bits M are unknown. Furthermore, ML approach is used also, and under a low SNR assumption to simplify the algorithm. The bits are here viewed as nuisance parameters. In [16], we can get rid of them by first computing the likelihood function for $a_k=(a_1, a_2, \dots, a_{M-1})$, τ and α , say $\Lambda(\tilde{\alpha}, \tilde{\alpha}, \tilde{\tau})$, and then averaging over the probability density of $\tilde{\alpha}$. This produces the marginal likelihood function for τ, α as [7]:

$$\Lambda(\tilde{\alpha}, \tilde{\tau}) = \int \Lambda(\tilde{\alpha}, \tilde{\alpha}, \tilde{\tau}) p(\tilde{\alpha}) d\tilde{\alpha} \quad (25)$$

From which the channel estimates are derived. As we have no specific knowledge of the data bits, except that they are independent and take on values zero and one with the same probability, we model $p(\tilde{\alpha})$ as:

$$p(\tilde{\alpha}) = \prod_{k=0}^{M-1} \frac{[\delta(\tilde{\alpha}_k) - \delta(\tilde{\alpha}_k - 1)]}{2} \quad (26)$$

Where $\delta(\tilde{\alpha})$ is the Dirac delta function. Reasoning as in the previous section by (DA) produces:

$$\Lambda(\tilde{\alpha}, \tilde{\alpha}, \tilde{\tau}) = \exp \left\{ \frac{1}{N_0} \left[2 \sum_{l=1}^{Lc} \tilde{\alpha} \sum_{k=0}^{M-1} z_k(\tilde{\tau}_l, \tilde{\alpha}_k) - ME_b \sum_{l=1}^{Lc} \tilde{\alpha}_l^2 \right] \right\} \quad (27)$$

This can be rearranged as:

$$\Lambda(\tilde{\alpha}, \tilde{\alpha}, \tilde{\tau}) = \exp \left\{ \frac{-ME_b}{N_0} \sum_{l=1}^{Lc} \tilde{\alpha}_l^2 \right\} \times \prod_{k=0}^{M-1} \exp \left\{ \frac{2}{N_0} \sum_{l=1}^{Lc} \tilde{\alpha}_l z_k(\tilde{\tau}_l, \tilde{\alpha}_k) \right\} \quad (28)$$

Next, averaging as indicated in (25) provides the desired result:

$$\Lambda(\tilde{\alpha}, \tilde{\tau}) = \exp \left\{ \frac{-ME_b}{N_0} \sum_{l=1}^{Lc} \tilde{\alpha}_l^2 \right\} \prod_{k=0}^{M-1} \left[\frac{1}{2} \exp \left\{ \frac{2}{N_0} \sum_{l=1}^{Lc} \tilde{\alpha}_l z_k(\tilde{\tau}_l, 0) \right\} + \frac{1}{2} \exp \left\{ \frac{2}{N_0} \sum_{l=1}^{Lc} \tilde{\alpha}_l z_k(\tilde{\tau}_l, 1) \right\} \right] \quad (29)$$

The drawback with this expression is that the maximization is computationally intense since it requires a numerical search over the multidimensional space spanned by $(\tilde{\alpha}, \tilde{\tau})$. Moreover, as the surface $\Lambda(\tilde{\alpha}, \tilde{\tau})$ might exhibit many spurious maxima, false locks would be possible with dramatic degradations in receiver performance. Some way out is needed to circumvent these obstacles. As a first step in this direction we choose to maximize $\log[\Lambda(\tilde{\alpha}, \tilde{\tau})]$ rather than $\Lambda(\tilde{\alpha}, \tilde{\tau})$ from (29), we have:

$$\log[\Lambda(\tilde{\alpha}, \tilde{\tau})] = \frac{-ME_b}{N_0} \sum_{l=1}^{Lc} \tilde{\alpha}_l^2 + \sum_{k=0}^{M-1} \log \left[\frac{1}{2} \exp \left\{ \frac{2}{N_0} \sum_{l=1}^{Lc} \tilde{\alpha}_l z_k(\tilde{\tau}_l, 0) \right\} + \frac{1}{2} \exp \left\{ \frac{2}{N_0} \sum_{l=1}^{Lc} \tilde{\alpha}_l z_k(\tilde{\tau}_l, 1) \right\} \right] \quad (30)$$

Next we assume that the SNR is so low that the following approximation can be made in (30):

$$\log \left[\frac{1}{2} \exp\{2x\} + \frac{1}{2} \exp\{2y\} \right] \approx x + y \quad |x|, |y| \ll 1 \quad (31)$$

Then, rearranging (30) we obtain:

$$\log[\Lambda(\tilde{\alpha}, \tilde{\tau})] \approx 2 \sum_{l=1}^{Lc} \tilde{\alpha}_l \frac{\sum_{k=0}^{M-1} z_k(\tilde{\tau}_l, 0) + z_k(\tilde{\tau}_l, 1)}{2} - ME_b \sum_{l=1}^{Lc} \tilde{\alpha}_l^2 \quad (32)$$

This result is rather interesting as it is quite similar to (21). In fact the two equations are identical, provided that $z_k(\tilde{\tau}_l, a_k)$ in (21) is replaced with $[z_k(\tilde{\tau}_l, 0) + z_k(\tilde{\tau}_l, 1)]/2$. It follows that the maximization method developed earlier is still valid with the indicated minor change [7].

4 Simulation Results

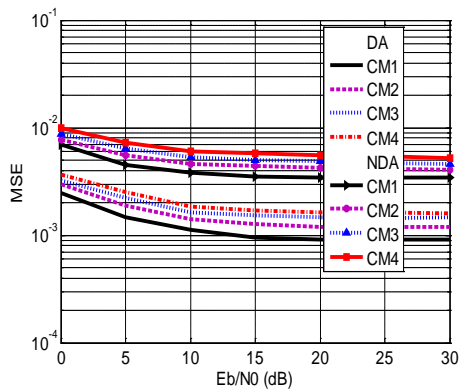
All results of performance evaluation based on our suppositions have been assessed using MATLAB simulation. Our simulations assume that

- Users have the same average power (perfect power control) such assuming in [7], [17].
- The energy of the channel impulse response is normalized to "1".

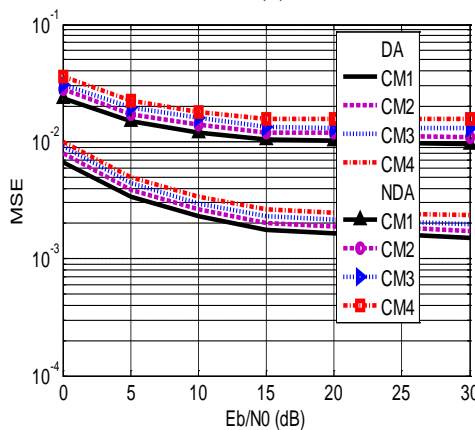
- The performances are evaluated over 100 channel realizations for each channel model (CM1, CM2, CM3, CM4) to have transparent results.

These results are given by applying a high bit rate, which is the inverse of one bit duration and equals 50Mbps. The sampling frequency is chosen $f_c=25\text{GHz}$, that means 25 samples per monocycle pulse according to [7][17], the number of frames in one bit is taken $N_f=2$, each impulse occupies one frame, and number of chips in one frame is $N_c=10$ to join ten users, c_j is the time hopping code associated at desired user in j^{th} frame and it is between $\{0, N_c-1\}$, the bit energy E_b is normalized to "1", the pulse duration $T_w=0.2$ ns and the modulation factor $\delta=0.2$ ns.

As can be seen from Fig 4.a and Fig 4.b, we evaluated the Mean Square Error (MSE) of the channel parameters (Gains, Delays) versus E_b/N_0 for a desired user. Moreover, the estimation sequence length is $M=100$ bits.



(a)



(b)

Fig.4 MSE of DA and NDA estimation for a) Gains estimates. b) Delays estimates

In the main, it can be shown that the MSE has a low degradation versus E_b/N_0 , because the UWB radio channel is largely affected by the multipath fading than the white Gaussian noise as confirmed by [9]. The DA estimation seems to be better than NDA as in [7]. Also, from $E_b/N_0=15\text{dB}$ the estimation of both gain and delay performs badly. The Fig.5 shows the BER versus E_b/N_0 for different channel models based on DA and NDA estimation. We made the AWGN channel in parallel with UWB channel models to show the marginal differences between them. It is clear that by increasing the model order, the BER is affected brusquely.

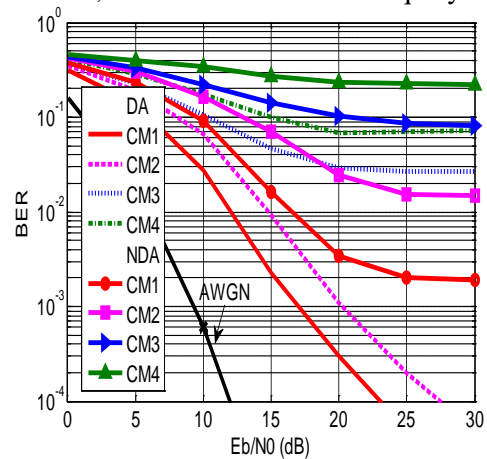
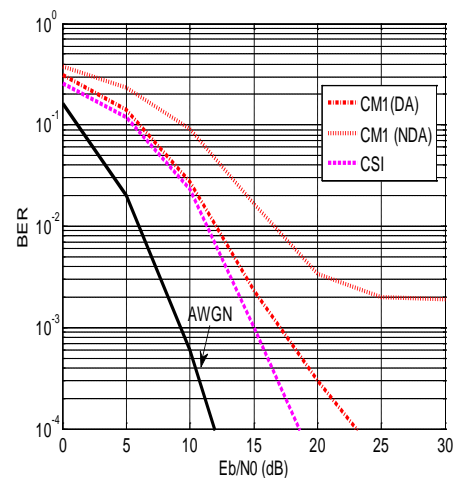
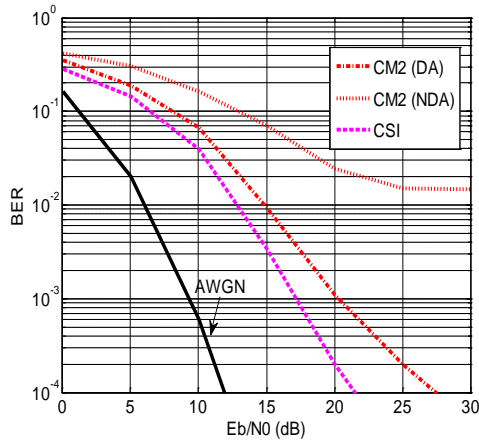


Fig.5 BER performance for DA and NDA estimation

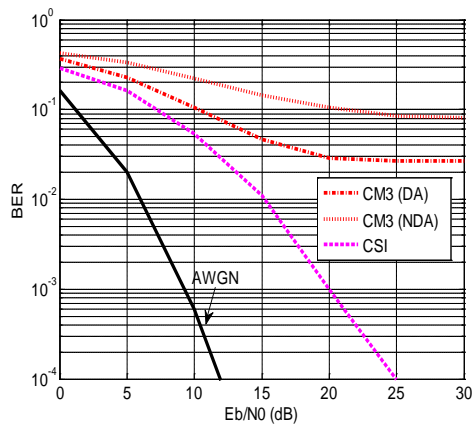
In order to clarify the performance of each channel model separately, in the following figures we plotted both the AWGN channel and the case of a perfect knowledge of the Channel State Information (CSI), which is assumed to be available at the receiver.



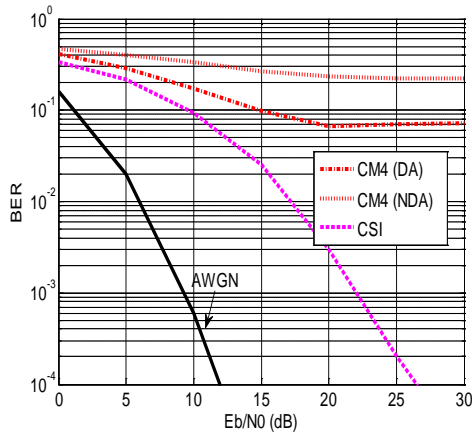
(a)



(b)



(c)



(d)

Fig.6 (a)-(b)-(c)-(d) BER performances of the channel Models compared with the AWGN channel and the CSI case

The Fig.7 shows the BER versus the number of users for the CM1 model, where up to ten users are implicated in this case. It is seen that the BER is affected in the two methods.

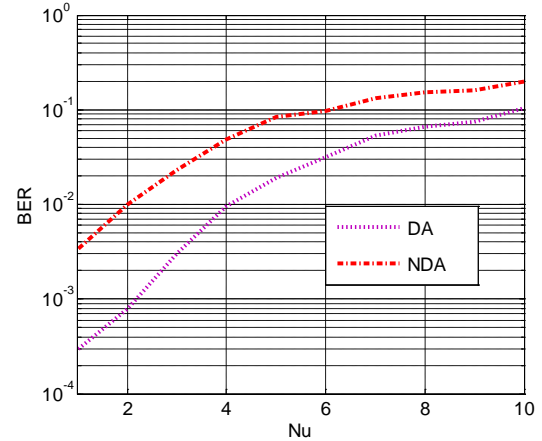


Fig.7 BER versus the number of users for CM1 model, $E_b/N_0=20\text{dB}$

5 Conclusion

In this work, a performance evaluation of TH-UWB transmission through proposed procedures has been made. Brief discussion on different blocks from the transmitter to the receiver has been implicitly shown. The IEEE 802.15.3a channel models have been used across all the results shown in this work. Besides this, the ML approach has been applied for UWB channel estimation using two methods, DA and NDA. The results make in evidence that the DA has more performances than the NDA, and when E_b/N_0 reaches 20 dB we have not more performance in the MSE of channel estimation. Furthermore, when the order of the channel model increases, the BER performance performs badly for all channel models, even if in the case of the multiuser access. Finally, this work can be viewed as a short survey paper on impulse radio TH-UWB transmission, where we have studied in this paper all the functional blocks of the TH-UWB transmission in multipath channels.

References:

- [1] M. K. A. Rahim, T. Masri, H. A. Majid, O. Ayop, F. Zubir, Design and Analysis of Ultra Wide Band Planar Monopole Antenna, *WSEAS Trans. Comm.*, Vol.10, No7, Jul 2011, pp. 212-221.
- [2] C. H. Cheng, G. J. Wen, Y. F. Huang, Hopfield Neural Network for UWB Multiuser Detection, *WSEAS Trans. Comm.*, Vol.8, No7, Jul 2009, pp. 578-587.
- [3] M. Renzo, and D. Leonardis, Timing Acquisition Performance Metrics of Tc-DTR UWB Receivers over Frequency-Selective

- Fading Channels with Narrow-Band Interference, *Wireless Commun*, Mar. 2010.
- [4] J. R. Foerster, M. Pendergrass, and A. F. Molisch, A channel model for ultrawideband indoor communication. In *International Symposium on Wireless Personal Multimedia Communication*. Oct. 2003
- [5] Y. Ishiyama, and T. Ohtsuki, Performance evaluation of UWB-IR and DS-UWB with MMSE-frequency domain equalization (FDE), In *Global Telecommunications Conference, IEEE GLOBECOM'04*, Vol. 5, Nov. 2004, pp. 3093-3097
- [6] Y. J. Chiu, Adaptive MMSE Rake-equalizer Receiver Design with Channel Estimation for DS - UWB systems, *WSEAS Trans. Comm.*, Vol.8, No.1, Jan 2009, pp. 196-205.
- [7] V. Lottici, A. D'Andrea, and U. Mengali, Channel Estimation for Ultra-wideband Communications, *IEEE J. Select. Area. Commun*, Vol.20, No.9, Dec. 2002, pp. 1638-1645.
- [8] B. Mielczarek, M. Wessman, and A. Svensson, Performance of coherent UWB rake receivers with channel estimators, in Proc. *IEEE VTC'03-Fall, Orlando, Florida*, Oct. 2003, pp. 1880-1884.
- [9] J. R. Foerster, Channel Modeling Sub-Committee Report (final), Tech. Rep. P802.15-02/490r1-SG3a, IEEE P802.15 Working Group for Wireless Personal Area Networks (WPANs), Feb. 2003.
- [10] Y. Li, A. F. Molisch, and J. Zhang, Channel Estimation and Signal Detection for UWB, in Proc. *Wireless Personal Multimedia Communications*, Vol.2, Oct. 2003, pp. 738-742
- [11] L. Zhao and A. M. Haimovich, Performance of Ultra-Wideband Communications in the Presence of Interference, in Proc. *IEEE Int. Conf. Communications (ICC'01)*, Helsinki, Finland, Jun. 2001, pp. 2948–2952
- [12] Win and R. A. Scholtz, Ultra-wide Bandwidth Time-hopping Spread-spectrum Impulse Radio for Wireless Multiple-access Communications, *IEEE Trans. Commun.*, Vol.48, Apr. 2000, pp. 679–691.
- [13] G. L. Turin, Introduction to Spread-Spectrum anti Multipath Techniques and Their Application to Urban Digital Radio, in Proc. *IEEE*, Vol.68, Mar. 1980, pp. 328–353.
- [14] A. Saleh and R. Valenzuela, A Statistical Model for Indoor Multipath Propagation, *IEEE JSAC*, Vol. SAC-5, No.2, Feb. 1987, pp. 128-137.
- [15] S. Verdù, *Multiuser Detection*, Cambridge, U.K.: Cambridge University Press, 1998.
- [16] S. M. Kay, *Fundamentals of Statistical Signal Processing: Estimation Theory*, Englewood Cliffs: Prentice-Hall, 1993.
- [17] A. Deleuze, Contributions à l'étude des systèmes ultra large bande par impulsions, *PhD thesis, the Superior National School of Télécommunications*, Paris 2006.